Revista Brasileira de Ciência do Solo

Division – Soil in Space and Time | Commission – Soil Survey and Classification

Genesis and Classification of Sodic Soils in the Northern Pantanal

Jairo Calderari de Oliveira Junior[(1)*], Mariane Chiapini[(2)], Alexandre Ferreira do Nascimento[(3)], Eduardo Guimarães Couto[(4)], Raphael Moreira Beirigo[(5)] and Pablo Vidal-Torrado[(2)]

[(1)] Universidade Federal do Paraná, Departamento de Solos e Engenharia Agrícola, Curitiba, Paraná, Brasil.
[(2)] Universidade de São Paulo, Escola Superior de Agricultura Luiz de Queiroz, Departamento de Ciência do Solo, Piracicaba, São Paulo, Brasil.
[(3)] Empresa Brasileira de Pesquisa Agropecuária, Embrapa Agrossilvipastoril, Sinop, Mato Grosso, Brasil.
[(4)] Universidade Federal do Mato Grosso, Departamento de Solos e Engenharia Rural, Cuiabá, Mato Grosso, Brasil.
[(5)] Universidade Federal da Paraíba, Centro de Ciências Agrárias, Areia, Paraíba, Brasil.

ABSTRACT: The simultaneous occurrence of high levels of exchangeable sodium percentage (ESP) and alkalinity in soils imposes restrictions on plant development and affects physical properties such as porosity, bulk density, permeability, and hydraulic conductivity. Although sodic soils are frequent in the flood plain of the São Lourenço River, northern Pantanal, Brazil, few studies focus on their formation and classification, especially with regard to specific processes and detailed classification into lower categorical levels by the different systems available. The aim of this study was to identify the predominant pedogenetic processes occurring in sodic soils of the flood plain of the São Lourenço River to understand their genesis and assess how taxonomic classification systems contemplate the variations in soil properties. Five profiles were selected in sites with different progressive stages of dissection from erosion (P1, P2, P3, P4, and P5). At each site, a pit was dug for morphological description of the profiles and for collecting samples for chemical, particle size, mineralogical, micromorphological, and chronological analyses. Each profile was classified according to the Soil Taxonomy, World Reference Base (WRB), and Brazilian Soil Classification System (SiBCS/ *Sistema Brasileiro de Classificação de Solos*). Argilluviation is the predominant process, with a localized and intense ferrolysis action in the E/Bt transition zones in profile P5. Soils showed signs of lithologic discontinuity. This makes it difficult to distinguish how much of the textural gradient is inherited from fluvial sedimentation processes and how much is the result of pedogenetic processes. In the most advanced stage of alteration, P5 had a paler color, thickening of the E horizon, and an abrupt and irregular transition entering the Bt horizon in the form of a “tongue”. When passing from the most preserved to the most eroded area, ferrolysis becomes more intense in the E/Bt transition, the electrical conductivity values decrease, and the ESP values increase, suggesting the sodification process. Under Soil Taxonomy criteria, P5 was classified as Natraqualf and the other profiles were classified as Natrudalf; under the WRB, however, all profiles were classified as Solonetz. The SiBCS exhibited variation at the Order level, with P5 classified as *Planossolo* and the others as *Luvissolo*. Despite an indication of different processes at the Order level, the SiBCS does not yet contemplate the sodic character in the studied *Luvissolos*. We propose inclusion of the sodic character at the Great Group level, as has already occurred with other SiBCS classes.

Keywords: *Planossolo*, *Luvissolo*, argilluviation, ferrolysis, micromorphology.

*** Corresponding author:**
E-mail: jairocalderari@gmail.com

Received: January 17, 2017
Approved: May 22, 2017

How to cite: Oliveira Junior JC, Chiapini M, Nascimento AF, Couto EG, Beirigo RM, Vidal-Torrado P. Genesis and classification of sodic soils in the northern Pantanal. Rev Bras Cienc Solo. 2017;41:e0170015.
https://doi.org/10.1590/18069657rbcs20170015

Copyright: This is an open-access article distributed under the terms of the Creative Commons Attribution License, which permits unrestricted use, distribution, and reproduction in any medium, provided that the original author and source are credited.

INTRODUCTION

A high exchangeable sodium percentage (ESP) in the soil is generally associated with a semi-arid climate due to higher rates of evapotranspiration than rainfall, which consequently decrease the leaching of Na^+, one of the chemical elements with greater soil mobility (Sumner and Naidu, 1998; Oliveira et al., 2009). Soils with these properties have limitations in plant development, since this ion competes with Ca^{2+} and Mg^{2+} for plant uptake. Physical properties are also deeply affected, since high ESP values associated with low values of electrical conductivity (EC <4.0 dS m^{-1}) promote strong dispersion of colloids that, in turn, migrate in depth, fill the porous spaces, decrease water infiltration, and increase B horizon density and susceptibility to water erosion (Rengasamy, 1997; Corrêa et al., 2003).

Most of the studies involving sodic soils in Brazil were developed in the Northeast region (Oliveira et al., 2009; Parahyba et al., 2009; Ferreira et al., 2016a,b), where a semi-arid climate predominates and rainfall rarely exceeds 800 mm yr^{-1}. This condition favors the incongruent dissolution of easily alterable primary minerals with high levels of Na^+ (e.g., albite) and disfavors leaching of the soil bases, resulting in the development of soils with a solodic or sodic character.

Some other regions in Brazil, with more humid climates, also have soils with high levels of Na^+, such as the northern Pantanal region (Nascimento et al., 2015); the genesis of these soils has been little studied. Unlike soils in the semi-arid region of Brazil, the sodic soils of the flood plain of the São Lourenço River, in the Pantanal region of Mato Grosso, occur mainly in the highest parts of the landscape (paleolevees) (Nascimento et al., 2015), which are used by wild or domesticated animals (beef cattle) as a refuge during the flood period (Silva and Girard, 2004). Thus, the importance of sodic soils in the Pantanal extrapolates their expression in terms of area, for they also play an important role in the ecology of the region, which may include intentional consumption by some wild animals (geophagy) to suppress nutritional deficiencies or to neutralize toxic compounds (Gilardi et al., 1999; Coelho, 2016).

In flood plains, the formation of sodic, alkaline, or saline soils is closely related to the process of concentration of river waters and their chemical properties (Furquim et al., 2010a; Furquim et al., 2010b). Rezende Filho et al. (2012) analyzed the chemical composition of the main rivers flowing into the Pantanal and observed that the São Lourenço river has alkaline-sodic waters that, when concentrated, favor control of Ca^{2+} by formation of carbonates, resulting in pH above 8.0 (Al-Droubi et al., 1980). The geomorphology of the flood plain of the São Lourenço River has several depositional lobes at different stages of dissection. Those lobes may form sodic soils at different stages and with different morphologies (Nascimento, 2012).

The taxonomic systems of soil classification are predominantly morphogenetic; that is, they are based on morphological properties and on the recognition of the processes responsible for soil formation (Arnold, 1983; Anjos et al., 2012), and are, ultimately, a reflection of the current knowledge of the soil (Krasilnikov et al., 2010). For the Soil Taxonomy (Soil Survey Staff, 2014) and the system of UN Food and Agriculture Organization - FAO (WRB, 2014), the process of accumulation of exchangeable sodium in the soil (sodification) is expressed by the Natric horizon, from the Latin *natrium* (Landon, 1991), or Arabic *natroon*, meaning salt (WRB, 2014). The properties of the natric horizon are similar in both systems, highlighting clay eluviation and the formation of a subsurface horizon with a more clayey content compared to the overlying one. It features coloration ranging from pale and yellowish to reddish, with prismatic, columnar, or block structure. It also shows evidence of clay illuviation: well-oriented clay coating features or clay "bridges" between grains of sand. Both systems consider that this horizon has ESP ≥15 %, resulting in poor water percolation and air circulation and weak structure that easily collapses. In addition, high levels of Na^+ can raise pH to values higher than 8.5.

In the Brazilian Soil Classification System (SiBCS), Na^+ concentrations in soil are divided into two ranges: one with ESP from 6 to 15 %, representing solodic character, and another with ESP ≥15 %, representing sodic character. Both are used as diagnostic characteristics;

that is, they can be present in more than one horizon and are not directly related to genesis of soil horizons. In general, the sodic character in the SiBCS is used in the third categorical level (Great Groups), as well as in Soil Taxonomy, and the solodic character is in the fourth categorical level (Subgroups). An exception is made in the *Planossolos* class, in which the sodic character is used in the second level (Suborder) as *Planossolo Nátrico*.

Due to the continental dimensions of Brazil, which are associated with a great diversity of soil formation factors (climate, relief, parent material, time period, and organisms), some diagnostic characteristics may not be satisfactorily contemplated by the SiBCS, and soil researchers and surveys must collaborate to improve the classification system (Ferreira et al., 2016a).

Thus, the aim of the present study was to identify the predominant pedogenetic processes occurring in sodic soils of the flood plain of the São Lourenço River in order to understand their genesis and assess how systems for taxonomic classifications contemplate the variations in soil characteristics.

MATERIALS AND METHODS

The study was conducted in the Private Natural Conservation Reserve (RPPN - *Reserva Particular do Patrimônio Natural*) belonging to the SESC Pantanal, located within the geographic coordinates 16° 32' - 16° 49' S and 56° 03'- 56° 26' W, in the municipality of Barão do Melgaço, northern Pantanal (Figure 1). Two important rivers of the Pantanal sedimentary basin exert considerable influence in the area, the Cuiabá River, defining the area to the west, and the São Lourenço River, which constitutes the eastern boundary. The climate of the region, according to the Köppen classification system, is Aw (Por, 1995), with monthly average temperature ranging from 22 to 32 °C. Annual rainfall is 1,100 mm, with an evapotranspiration potential of 1,400 mm annually, resulting in water deficit of 300 mm per year. The most striking feature of the Pantanal is the annual inundation of its plains, which in the area studied occurs from October to April, as a result of low local declivity and a large volume of water coming from the plateaus surrounding the Pantanal (Assine and Soares, 2004). The soils found in the RPPN are *Gleissolos*, *Neossolos*, *Cambissolos*, *Plintossolos*, *Planossolos*, and *Luvissolos* (Beirigo et al., 2011); these last two are generally and closely associated in the landscape.

Selection of the points sampled was based on the geomorphic classification of the flood plain of the São Lourenço River, performed by Nascimento (2012). This author identified higher areas (paleolevees) and lower areas (floodplains) in five different stages of erosion. The areas in a more advanced stage of erosion were considered older and their soils were more altered by pedogenetic processes (evolved). In all, five study sites were selected, one in each geomorphic unit, for opening profiles, morphological description, and sample collection (Figures 2 and 3). Morphological description was based on a guide prepared by the FAO (2006). Disturbed samples of each horizon were collected, dried, and passed through a sieve with an aperture of 2 mm to obtain air-dried fine earth (ADFE), which was then subjected to routine chemical and particle size analysis. The particle size analysis was performed with a hydrometer (Donagema et al., 2011) using a solution of 1 mol L^{-1} NaOH and 0.015 mol L^{-1} sodium hexametaphosphate ($Na_{16}P_{14}O_{43}$) as dispersing agents. For sand fractioning, the following ranges were used: very coarse sand (2 to 1 mm); coarse sand (1 to 0.5 mm); medium sand (0.5 to 0.25 mm); fine sand (0.25 to 0.125 mm); and very fine sand (0.125 to 0.05 mm). To allow observation of possible lithologic discontinuities, graphs of the sand fraction distribution in relation to the total amount of sand were drawn up, and proportions between the coarse and medium (c/m), coarse and fine (c/f), and medium and fine (m/f) fractions were calculated. According to WRB criteria (WRB, 2014), lithologic discontinuity between directly overlapping horizons is characterized when there is a variation of at least 25 % between the proportions, as well as an increase in the absolute content of one of the sand fractions of at least 5 % of the ADFE.

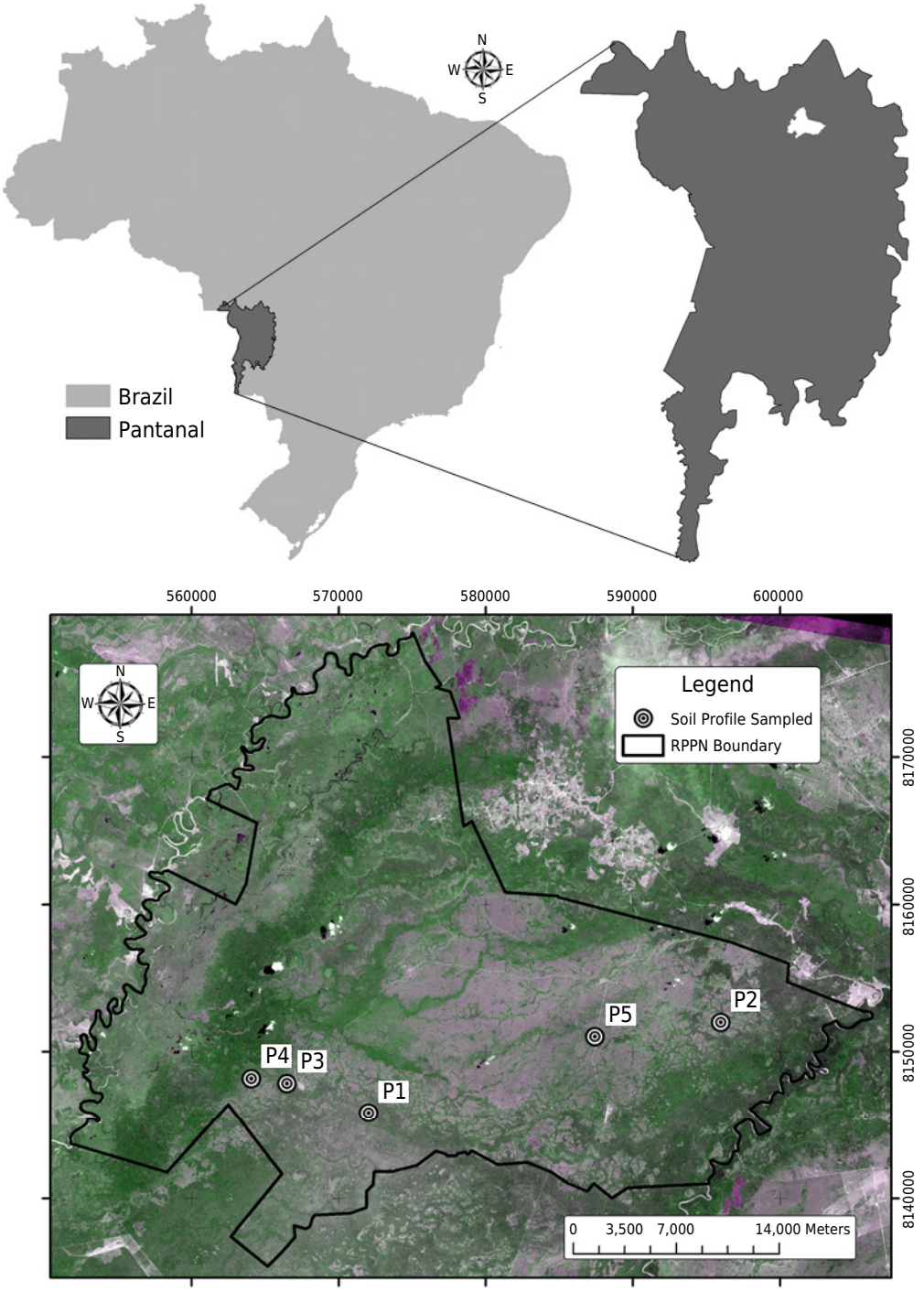

Figure 1. Location of the Pantanal region within Brazilian territory and the RPNN SESC Pantanal (white area) within the Pantanal. Distribution of the five profiles (P1, P2, P3, P4, and P5) within the SESC Pantanal RPPN.

Soil pH values were determined in water (1:2.5); Al^{3+} was extracted with 1 mol L^{-1} KCl and determined by titration with NaOH; for H+Al, calcium acetate was used as an extractor and was determined by titration with NaOH; Ca^{2+} and Mg^{2+} were extracted with 1 mol L^{-1} KCl and determined by atomic absorption; K^{+} and Na^{+} were extracted by Mehlich-1 and were determined by a flame spectrophotometer (Donagema et al., 2011).

For mineralogical analysis, samples of the Bt horizon of each profile were used. The organic matter of the samples was eliminated with the addition of 30 % H_2O_2, and Fe oxides were eliminated with dithionite-citrate-bicarbonate (DCB) in a water bath at 80 °C for 30 min at each extraction, repeating the procedure three times. This procedure avoids the interference

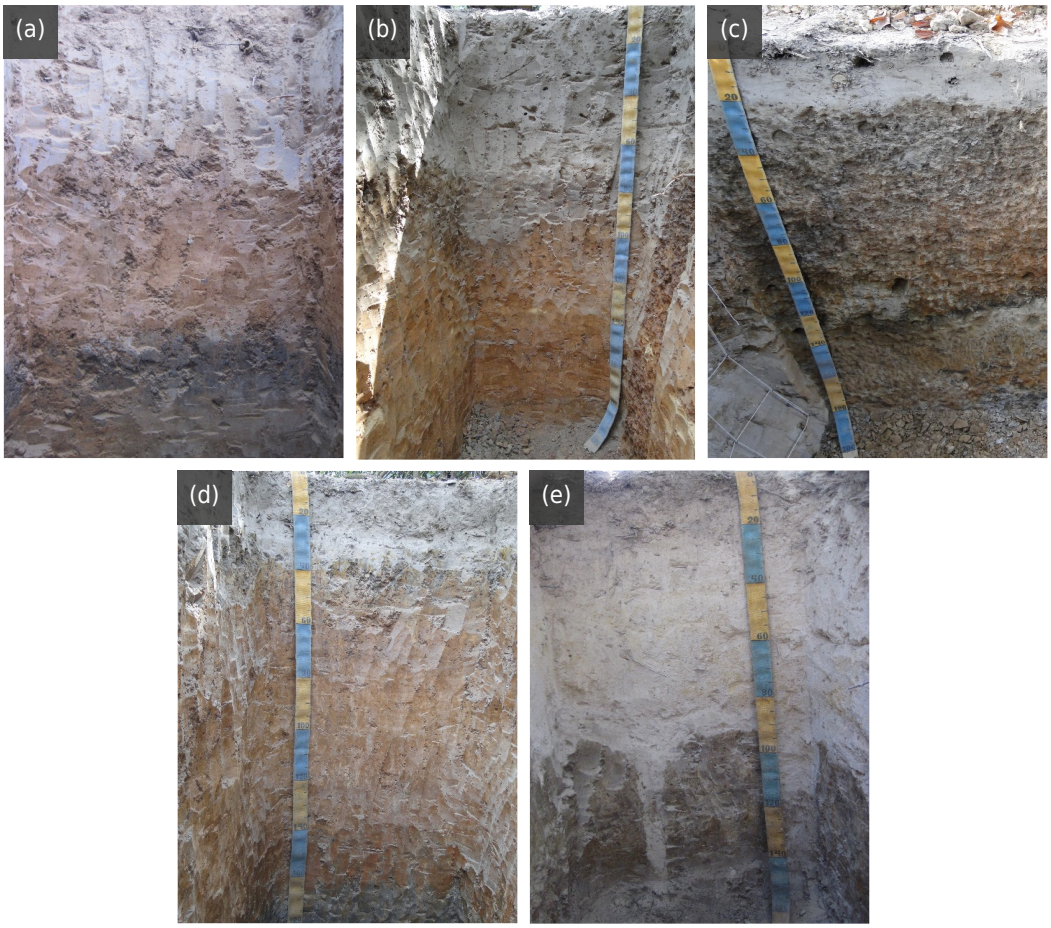

Figure 2. Soil profiles of points P1 (a), P2 (b), P3 (c), P4 (d), and P5 (e). All profiles had abrupt textural change, a B horizon with high chroma, with the exception of P5 which featured pale colors due to lower permeability, and a thicker E horizon entering the B horizon in "tongue" format.

of Fe oxides in identification and interpretation of phyllosilicates in X-ray diffractograms (XRD) (Jackson, 1979). Separation of the sand fraction from the silt + clay fractions was performed by sieving, and the clay was later separated from the silt by decantation, following Stokes' law. After obtaining the clay, it was fractionated into fine (<0.2 µm) and coarse (0.2-2.0 µm) clay by means of successive centrifugations (4,100 rpm for 21 min) in a sodium carbonate solution ($NaCO_3$); the supernatant (<0.2 µm) was siphoned and subsequently lyophilized. The samples were subjected to a treatment with saturation by Mg^{2+} (Mg 25 °C) and then solvated with ethylene glycol (Mg EG). In both treatments, the material was used in setting up XRD oriented slides in a Rigaku Miniflex II diffractometer, equipped with a graphite-monochromated Cu Kα, operated at a voltage of 15 kV and 10 mA of current, at a step of 0.02° 2θ and a speed of 1 s per step, in the range of 3° to 30° 2θ.

To prepare thin section for subsequent micromorphological description, undisturbed blocks of samples were collected from the main B horizons of each profile. After being completely dried, the blocks were impregnated in a vacuum system using a solution containing a mixture of polyester resin (Arazyn 1.0 - Ashland) and styrene monomer in a 1:1 proportion, plus Tinopal OB (BASF®) fluorescent pigment in all samples and a catalyst (Butanox), as described by Murphy (1986). After complete hardening, the block was cut in pieces with dimensions of 18 × 70 × 50 mm, continuing to polish one side up to a thickness of approximately 30 µm, which was bonded in a 5 × 8 cm glass slide for examination under a petrographic microscope.

Some samples of a sandy texture at the base of the P2, P3, and P5 profiles were collected in PVC tubes and dated using optically stimulated luminescence (OSL) at the *Laboratório de Datação, Comércio e Prestação de Serviços LTDA* in São Paulo, Brazil, following the

Figure 3. The areas where profiles P1(a); P2 (b); P3 (c); P4 (d); and P5 (e) were collected. The presence of Acuri (*Attalea phalerata*), an indicator plant for sodic soils, is observed in all locations. In P5, shrub/arboreal vegetation marks the sudden transition between the floodplain and higher lands. Geophagy of the sodic material is frequently observed (f) - image courtesy of Coelho IP.

single-aliquot-regenerative dose (SAR) protocol proposed by Wallinga et al. (2000). It was not possible to collect samples of the other profiles for dating since they did not have a sandy layer beyond 0.50 m depth. In the P2 and P3 profiles, calcium carbonate nodules were observed in the middle of the Bt horizon; however, nodule separation from the soil matrix was only possible in the P2 profile. The nodules were sent to the laboratory of Beta Analytic Inc. for ^{14}C dating by accelerator mass spectrometry (AMS).

To compare how the horizons and diagnostic properties are used by the main soil classification systems, soil profiles were taxonomically classified using the SiBCS (Santos et al., 2013), Soil Taxonomy (Soil Survey Staff, 2014), and FAO (WRB, 2014).

RESULTS

Morphology and dating

With the exception of the P1 profile, all others had an E horizon, with high values and low chroma (Table 1 and Figure 1). The colors of the soils ranged from the hue 7.5YR to 10YR, suggesting the predominance of goethite as iron oxide (Kämpf and Curi, 2000).

Table 1. Morphological description of the profiles opened at the five sites studied: P1, P2, P3, P4, and P5

Prof[1]	Hz[2]	Depth	Dis[3]	Top[4]	Col[5]		Mot[6]		Nod[7]	Structure[8]	Consistence[9]			Coating[10]
					Matiz	H/C	Matiz	H/C			Dry	Moist	Wet	
		m												
P1	A	0.35	Ab	Sm	10YR	6/4	-	-	-	ST, ME, GR	SO	FR	SST/SPL	-
	2Btn1	0.70	Gr	Sm	7.5YR	4/6	-	-	-	ST, CO, PR	HA	FI	VST/VPL	c/d
	3Btn2	1.05	Ab	Sm	7.5YR	6/6	-	-	-	ST, CO, PR	HA	FI	ST/PL	f/vf
	4Cn	2.00+	-	-	7.5YR	4/3	-	-	-	MA	SHA	VFR	SST/SPL	-
P2	A	0.25	Gr	Sm	10YR	4/2	-	-	-	WE, VF, GR	LO	LO	NST/NPL	-
	E	0.65	Ab	Sm	7.5YR	6/3	-	-	-	SG	LO	LO	NST/NPL	-
	2Btn1	1.00	Gr	Sm	7.5YR	4/6	-	-	-	ST, ME, PR	VHA	VFI	VST/VPL	c/vf
	2Btn2	1.50	Gr	Sm	7.5YR	5/8	-	-	-	ST, ME, PR	VHA	FI	VST/VPL	c/d
	2Btnk	2.00+	-	-	7.5YR	6/8	-	-	k	ST, CO, PR	HA	FI	VST/VPL	c/d
P3	An	0.10	Gr	Sm	7.5YR	7/1	-	-	-	WE, VF, GR	LO	LO	NST/NPL	-
	En	0.25	Ab	Sm	10YR	8/1	-	-	-	SG	LO	LO	NST/NPL	-
	2Btn	0.60	Gr	Ir	7.5YR	5/3	5YR	4/5	-	ST, VC, PR	VHA	VFI	VST/VPL	a/f
	3Btnk	1.15	Gr	Ir	7.5YR	5/6	5YR	4/6	k	ST, VC, PR	HA	FI	VST/VPL	a/f
	4Cgn1	1.30	Ab	Ir	7.5YR	6/2	5YR	5/6	-	MA	HA	FR	SST/SPL	-
	5Cgn2	1.80+	-	-	7.5YR	6/2	5YR	5/6	-	MA	HA	FR	SST/SPL	-
P4	A	0.15	Gr	Sm	10YR	6/4	-	-	-	WE, VF, GR	LO	LO	NST/NPL	-
	E	0.35	Ab	Sm	10YR	8/1	-	-	-	SG	LO	LO	NST/NPL	-
	Btn1	1.20	Gr	Sm	7.5YR	4/6	-	-	-	ST, ME, SB	VHA	VFI	VST/VPL	c/d
	Btn2	1.55	Gr	Sm	7.5YR	5/6	-	-	-	ST, VC, SB	VHA	VFI	VST/VPL	c/d
	2Cgn	2.00+	-	-	7.5YR	4/2	-	-	-	MA	VHA	FI	VST/VPL	-
P5	A	0.20	Gr	Sm	7.5YR	7/1	-	-	-	SG	LO	LO	NST/NPL	-
	En	1.00	Ab	Br	10YR	8/1	-	-	Mn	SG	LO	LO	NST/NPL	-
	2Btgn1	1.30	Gr	Ir	7.5YR	4/1	10R	4/8	Mn	ST, ME, SB	HA	FI	ST/PL	a/vf
	2Btgn2	1.60+	-	-	10YR	4/1	10R	4/8	-	ST, ME, SB	HA	VFI	VST/VPL	c/d

[1] Profile. [2] Horizon. [3] Distinctness: Ab = abrupt, Gr = gradual. [4] Topography: Sm = smooth, Ir = irregular, Br = broken. [5] Soil matrix color notation in Munsell Soil Chart Color: H = hue, C = Chroma. [6] Mottle color notation in Munsell Soil Chart Color. [7] nodule: k = carbonate, Mn = manganese and iron. [8] Structure: strong (ST), massive (MA), weak (WE), single grain (SG), medium (ME), coarse (CO), very fine (VF), very coarse (VC), granular (GR), prismatic (PR), subangular blocky (SA). [9] Consistence: soft (SO), hard (HA), slightly hard (SHA), loose (LO), very hard (VHA), friable (FR), firm (FI), very friable (VFR), very firm (VFI), slightly sticky (SST), very sticky (VST), sticky (ST), non-sticky (NST), slightly plastic (SPL), very plastic (VPL), plastic (PL), non-plastic (NPL). [10] Coating: common (c), distinct (d), faint (f), very few (v), and abundant (a).

In the uppermost horizons, which had a more sandy content than underlying horizons (Table 2), the structures appeared in single grains. The C horizons had a massive structure. The Bt horizons, with clay content ranging from 225 to 475 g kg^{-1}, had a strong grade of structure, ranging in size from medium to very large, and of prismatic type for P1, P2, and P3; blocky subangular structures were observed for P4 and P5 (Table 1). In the P5 profile, a large concentration of Fe and Mn nodules was observed in the E and Btgn1 horizons.

The dating of the quartz material by OSL from the samples collected in the P2, P3, and P5 profiles indicated that they last received light about 52,400; 21,500; and 40,000 years BP, respectively (Table 2). The AMS dating of calcium carbonate collected in P2, indicated an average age of 660 years BP.

Chemical properties and particle size analysis

Except for the P5 profile, the pH values of the subsurface horizons were neutral to alkaline, in some cases exceeding 9.0 (Table 3). The pH values were slightly acidic for profile P5, ranging from 5.3 to 6.6. The EC values showed a decreasing trend from P1 to P5, with the highest value for the 2Btn1 of P1 (1.79 mS m^{-1}) and the lowest for the 2Btgn2 of P5

Table 2. Soil particle analysis, horizons sampled for making thin sections, dating, and determining ages

Prof[1]	Hz[2]	Clay	Silt	Total sand	Thin[3]	Dating[4]	Age[5]
		g kg^{-1}					
P1	A	15	27	58	-	-	-
	2Btn1	33	37	30	X	-	-
	3Btn2	23	2	75	-	-	-
	4Cn	18	43	39	-	-	-
P2	A	10	29	61	-	-	-
	E	10	29	61	-	-	-
	2Btn1	30	37	33	X	-	-
	2Btn2	28	43	30	-	-	-
	2Btnk	30	57	13	X	AMS/OSL	660/52,400
P3	An	9	24	67	-	-	-
	En	8	7	86	-	-	-
	2Btn	26	33	41	-	-	-
	3Btnk	28	21	51	X	-	-
	4Cgn1	9	6	85	-	-	-
	5Cgn2	16	2	82	-	OSL	21,500
P4	A	5	17	78	-	-	-
	E	5	21	74	-	-	-
	Btn1	30	52	22	X	-	-
	Btn2	35	58	7	-	-	-
	2Cgn	45	25	30	-	-	-
P5	A	18	2	80	-	-	-
	En	15	5	80	X	-	-
	2Btgn1	38	8	54	X	-	-
	2Btgn2	48	8	44	-	OSL	40,000

[1] Profile. [2] Horizon. [3] Thin section: horizons from which the undisturbed sample was collected. [4] Dating: corresponding horizon from which sandy material was collected for OSL dating or carbonate material was collected for AMS dating. [5] Age in years measured by AMS/OSL method.

(0.23 mS m^{-1}). However, the highest values were not enough to identify horizons with salic or saline character (Santos, 2013). With the exception of the P3 profile, the other profiles had zero or very low H+Al values. For most of the horizons, the Ca^{2+} values were lower than those of Mg^{2+}, a situation observed in some sodic horizons of soils in the Northeast Region of Brazil (Oliveira et al., 2009; Ferreira et al., 2016b).

The K^+ contents were higher than Na^+ contents only in the surface horizons of the P2, P4, and P5 profiles and in the E horizon of the P2 and P4 profiles. Taking the B horizons as a reference, ESP values showed a tendency to increase from P1 (20 %) to P5 (51 %), with the highest value observed in the Btn1 of P4 (60 %), identifying the sodic character. In P5, the sodic character is observed even in the eluvial horizon (E), with saturation by Na^+ of 33 % in the exchange complex (Table 3).

In all profiles, the B horizons had higher clay content (Bt), but with values rarely exceeding 375 g kg^{-1} (Table 2). High levels of silt were observed in the Bt horizon of P2 and P4, whereas the values were relatively low in P5. In the other horizons and profiles, there was a large contribution of very fine and fine sand fractions, while the quantity of coarse or very coarse sand fractions were very low or zero. The distribution of the different sand fraction classes (Figure 4) showed that for the P3 and P5 profiles, all horizons have the same pattern, while for P1, only the 2Btn horizon exhibited a pattern slightly different from the others, with very fine sand predominating. For P2 and P4, the A and E horizons

Table 3. Chemical analysis of the profiles studied

Prof[1]	Hz[2]	pH(H_2O)	EC	C_{org}	H+Al	Al^{3+}	Ca^{2+}	Mg^{2+}	Na^{+}	K^{+}	S	CEC	T clay	V	ESP
			dS m^{-1}	g kg^{-1}	$cmol_c$ kg^{-1}									%	
P1	A	6.2	0.74	24	0.0	0.0	2.0	1.3	0.1	0.1	3.5	3.5	-	100	3
	2Btn1	8.8	1.58	11	0.0	0.0	3.5	4.4	2.2	0.9	11	11	34	100	20
	3Btn2	8.8	1.79	8	0.0	0.0	3.7	5.5	3.0	1.2	13.4	13.4	60	100	22
	4Cn	9.1	0.95	5	0.0	0.0	0.7	2.2	1.5	0.7	5.1	5.1	30	100	28
P2	A	6.6	0.41	24	0.0	0.0	8.5	3.3	0.1	0.8	12.7	12.7	-	100	0
	E	8.0	0.04	5	0.0	0.0	1.1	1.9	0.2	0.6	3.8	3.8	-	100	26
	2Btn1	8.9	0.76	9	0.0	0.0	1.4	4.4	2.1	1.8	9.7	9.7	32	100	22
	2Btn2	9.5	0.87	5	0.0	0.0	1.4	3.3	2.8	1.2	8.7	8.7	32	100	32
	2Btnk	9.7	1.15	6	0.0	0.0	1.8	5.5	5.4	1.8	14.5	14.5	48	100	38
P3	An	6.5	0.46	10	1.2	0.0	2.3	2.4	0.5	0.4	5.6	6.8	-	82	8
	En	6.7	0.17	5	1.0	0.0	0.5	1.4	0.3	0.3	2.5	3.5	-	71	9
	2Btn	9.1	0.49	5	0.2	0.0	2.8	4.8	4.4	0.7	12.7	12.9	49	98	34
	3Btnk	8.8	0.20	3	0.2	0.0	2.5	4.9	4.5	0.8	12.7	12.9	47	98	35
	4Cgn1	7.9	0.11	5	0.2	0.0	0.4	2.2	1.6	0.2	4.4	4.6	51	96	35
	5Cgn2	6.7	0.07	5	0.8	0.5	0.2	2.6	1.9	0.2	4.9	5.7	35	86	33
P4	A	6.2	0.34	20	0.4	0.1	0.4	0.2	0.0	0.1	0.7	1.1	-	64	2
	E	7.1	0.05	4	0.0	0.0	0.2	0.1	0.0	0.1	0.4	0.4	-	100	5
	Btn1	8.9	0.71	9	0.0	0.0	1.9	2.2	6.5	0.2	10.8	10.8	36	100	60
	Btn2	8.7	0.60	6	0.0	0.0	3.0	4.4	7.9	0.2	15.5	15.5	44	100	51
	2Cgn	8.2	0.63	6	0.0	0.0	2.8	2.2	7.5	0.2	12.7	12.7	28	100	59
P5	A	5.3	0.21	16	0.5	0.3	1.1	1.1	0.0	0.6	2.8	3.3	-	85	0
	En	6.6	0.12	7	0.0	0.0	1.1	0.0	0.8	0.5	2.4	2.4	-	100	33
	2Btgn1	6.3	0.45	8	0.0	0.1	1.1	3.3	3.5	2.6	10.5	10.5	19	100	49
	2Btgn2	6.0	0.23	8	0.0	1.9	0.0	2.2	2.5	0.8	5.5	5.5	11	100	51

[1] Profile. [2] Horizon. EC: electrical conductivity in saturated soil-paste; pH(H2O): soil:solution relation 1:2.5 (v/v); C_{org}: organic carbon extracted by Walkley and Black; H+Al extracted by calcium acetate 0.5 mol L^{-1}; Al^{3+}, Ca^{2+}, and Mg^{2+} extracted by 1 mol L^{-1} KCl; K^{+} and Na^{+} extracted by Mehlich-1; S: sum of basic cations (Ca^{2+}, Mg^{2+}, K^{+}, and Na^{+}); CEC: cation exchange capacity; T clay: exchange capacity of the clay fraction; V: base saturation [(S/CTC)×100]; and ESP: exchangeable sodium percentage, calculated in CEC.

had a similar pattern but it was different from the underlying B horizon. However, using the lithologic discontinuity criteria applied by the FAO (WRB, 2014), all the profiles studied had lithologic discontinuity in the transition between at least two horizons (Table 4).

Mineralogy and micromorphology

The XRDs of the fine clay fraction of all Bt horizons indicate the presence of kaolinite, smectite, and illite, also in the P5 profile, characterized as being in a more advanced stage of alteration (Figure 5). In the XRD of P5, the kaolinite *001* reflection was similar to the XRD from other horizons but with a higher intensity, indicating a higher degree of crystallinity of the mineral in this horizon (Oliveira Junior et al., 2014). In the XRDs, with the exception of the B horizon of the P5 profile, the reflections of the *001* plane of kaolinite exhibited asymmetry in all the samples. Similar behavior was observed for the reflections of the *001* plane of smectite when saturated with Mg^{2+}, which, after ethylene glycol solvation, was dismembered in two others planes, one peak typical of smectite and the other peak typical of illite.

Micromorphological description showed that the process of clay illuviation is present in all the Bt horizons studied (Table 5). In some horizons, illuviation even occurs between the calcium carbonate nodules (Figure 6). In the transition between the En and 2Btgn1

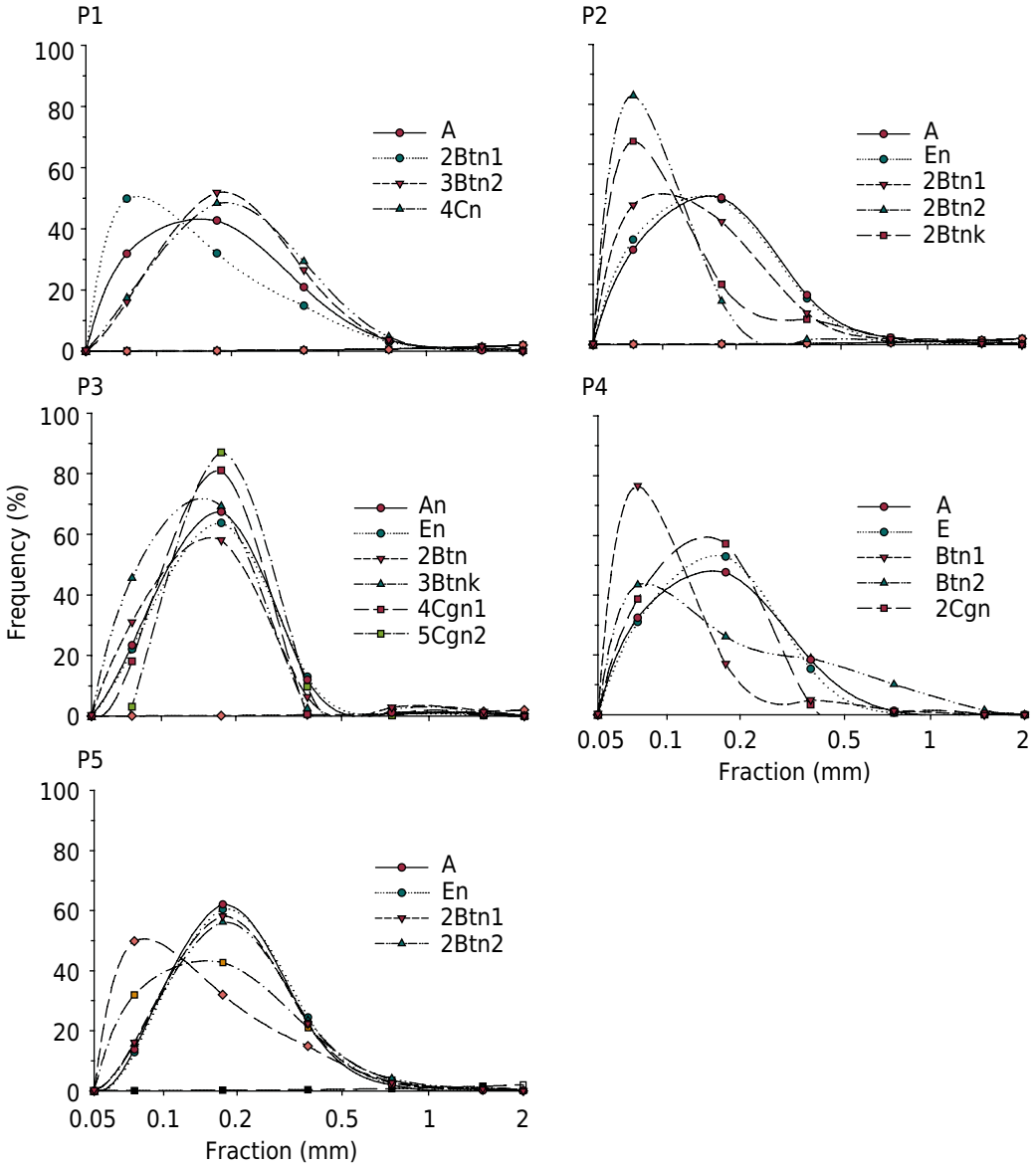

Figure 4. Relative distribution of the sand fractions (very fine, fine, medium, coarse, and very coarse) of each horizon in the profiles.

horizons of the P5 profile, the more intense eluviation/illuviation process can be observed and part of the eluviated matrix with relative concentration in quartz. Thus, for purposes of description, the thin section of the 2Btgn1 horizon of the P5 profile was divided into two zones (Figure 7b), porphyric type and gefuric type (Bullock et al., 1985; Stoops, 2003). In the transition between these two zones, there are cavities with clay and Fe coatings, and some have mamelonar walls, suggesting a coalescence of cavities (Figure 7c) resulting from ferrolysis (Vidal-Torrado et al., 1999; Oliveira Junior et al., 2017). The porphyric pattern was also observed in the samples of the Bt horizons of the P2 and P4 profiles, whereas this pattern was described as chitonic for the P1 profile and as gefuric for P3 (Table 5).

With the exception of the P4 profile, all the horizons sampled had textured features containing Fe, such as hypocoatings and coatings. Highly weatherable primary minerals were only observed in the 3Btnk horizon of the P3 profile, while in the other horizons and profiles studied the skeleton is exclusively made up of quartz.

Classification

Due to the presence of the B *plânico* horizon, with abrupt textural change and pale color, P5 was classified as a *Planossolo* in the first categorical level (Order) in the

Table 4. Fractionation of the sand classes, sand contents ratios, and their variation in percentage to determine lithologic discontinuity

Prof[1]	Hz[2]	Sand[3]						c/m		c/f		m/f	
		total	vf	f	m	c	vc	prop[4]	%[5]	prop	%	prop	%
		%											
P1	A	58	19	25	12	2	1	0.17	33*	0.08	20	0.48	17
	2Btn1	30	15	10	4	1	0	0.25	40*	0.10	23	0.40	22
	3Btn2	75	12	39	20	3	1	0.15	18	0.08	27*	0.51	11
	4Cn	39	7	19	11	2	0	0.18	-	0.11	-	0.58	-
P2	A	61	19	30	10	1	0	0.10	10	0.03	3	0.32	7
	E	61	21	30	9	1	0	0.11	67*	0.03	53*	0.30	29*
	2Btn1	33	15	13	3	1	0	0.33	-	0.07	-	0.21	14
	2Btn2	30	25	4	1	0	0	0.00	-	0.00	-	0.25	25
	2Btnk	13	9	3	1	0	0	0.00	-	0.00	-	0.33	-
P3	An	67	16	45	8	1	1	0.14	36	0.02	22	0.16	19
	En	86	19	55	11	1	0	0.09	73*	0.02	58*	0.20	35*
	2Btn	41	13	24	3	1	1	0.33	-	0.04	-	0.13	74*
	3Btnk	51	23	35	1	1	0	0.00	0	0.00	0	0.03	57*
	4Cgn1	85	15	69	1	0	0	0.00	0	0.00	0	0.01	87*
	5Cgn2	82	3	72	8	0	0	0.00	-	0.00	-	0.11	-
P4	A	78	25	37	14	1	0	0.07	21	0.03	3	0.37	23
	E	74	23	39	11	1	0	0.09	-	0.03	-	0.28	11
	Btn1	22	17	4	1	0	0	0.00	-	0.00	-	0.25	50
	Btn2	7	3	2	1	1	0	1.00	-	0.50	-	0.50	88*
	2Cgn	30	12	17	1	0	0	0.00	-	0.00	-	0.06	-
P5	A	80	11	50	18	2	0	0.11	10	0.04	2	0.37	12
	En	80	10	49	20	2	0	0.10	40*	0.04	35*	0.42	7
	2Btgn1	54	9	32	12	2	0	0.17	17	0.06	19	0.39	3
	2Btgn2	44	7	25	10	2	0	0.20	-	0.08	-	0.40	-

[1] Profile. [2] Horizon. [3] Sand content in fine-earth fraction in total sand (total), very fine (vf), fine (f), medium (m), coarse (c), and very coarse (vc). [4] Proportion between coarse and medium classes (c/m), coarse and fine (c/f), medium and fine (m/f). [5] Variation of proportions between horizons in the line and underlying horizon. * Lithologic discontinuity between horizons according to the FAO (WRB, 2014).

SiBCS and, as ESP is higher than 15 %, it was classified in the second level (Suborder) as *Nátrico* (Table 6). For the other profiles, the subsurface increase in clay, forming the textural B horizon, associated with high activity clay and eutrophic character, composed the diagnostic criteria for classification as *Luvissols* at the first level. As they had a chromic character, profiles P1, P2, P3, and P4 were classified as *Crômico* at the second categorical level. At the third categorical level, since the sum of the thicknesses of the A+B or A+E+B horizons exceeded 0.80 m in thickness, they were classified as *Pálico*. Due to the mottles observed in the 2Btn and 3Btnk horizons of the P3 profile, they were classified at the fourth categorical level as *planossólico*. Profiles P1, P2, and P4 did not show variegated color or nodules but, due to abrupt transition, they were classified at the fourth level as *abrupto*.

By Soil Taxonomy, all soils, at the Order level, were identified as Alfisols, due to base saturation, a clay increase with depth, and formation of a textural B horizon. At the suborder level, P5 was identified as an aquic moisture regime, while others were classified as ustic, and at the Great Group level, all profiles were identified as Natric.

The WRB classification identified all soils as Abruptic Solonetz, due to the increase in clay and the high ESP value. Among the qualifiers, all the soils were classified as Hypernatric, Magnesic, and Cutanic (Table 6).

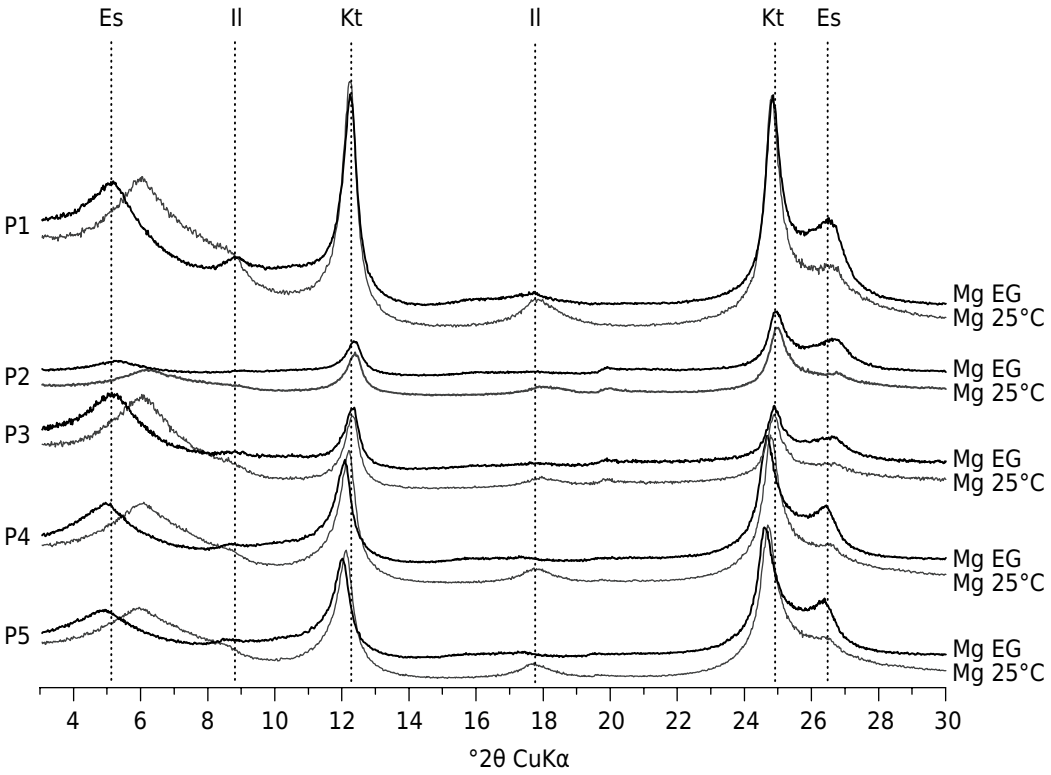

Figure 5. Diffractograms of the fine clay samples of the B horizons, saturated with Mg (Mg 25 °C) and solvated with ethylene glycol (Mg EG). In all profiles (P1, P2, P3, P4, and P5), there is the presence of crystallinity of kaolinite (Kt) in a greater degree, followed by 2:1 clay minerals, such as smectite (Es) and illite (Il).

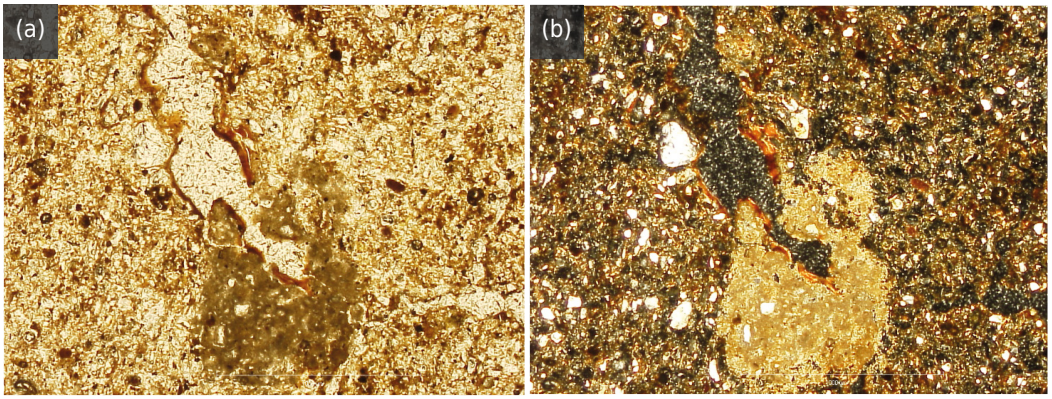

Figure 6. Photomicrography of the 2Btnk horizon of P2 and clay coatings (arrow) in the middle of a calcium carbonate (Ca) nodule fractured in flat light (PPL) (a); and with crossed nicols (XPL) (b), indicating that the clay coating is more recent and, hierarchically, is the most active.

DISCUSSION

Soil properties and pedogenetic processes

The ages of the sandy sediments obtained by OSL places the profiles studied in the Pleistocene (Table 2), but the chronological sequence does not correspond to the sequence of geomorphic evolution described by Nascimento (2012) for the different geomorphic units. This anachronism resulted from the evolution of the units, which is closely related to the erosive intensity imposed by the river. This erosive intensity can alternate according to the climatic and hydropedological conditions in different epochs. However, comparing the dates with the environmental variations described by Corradini and Assine (2012) and by McGlue et al. (2012), it can be observed that these profiles passed through a drier

period with higher sedimentation that were favorable to concentration of ions in the soil and the formation of saline and sodic characters. Because the current climate conditions are more humid, the incision of the rivers is more accentuated (Corradini and Assine, 2012) and, consequently, erosion processes predominate, which are the main aspect

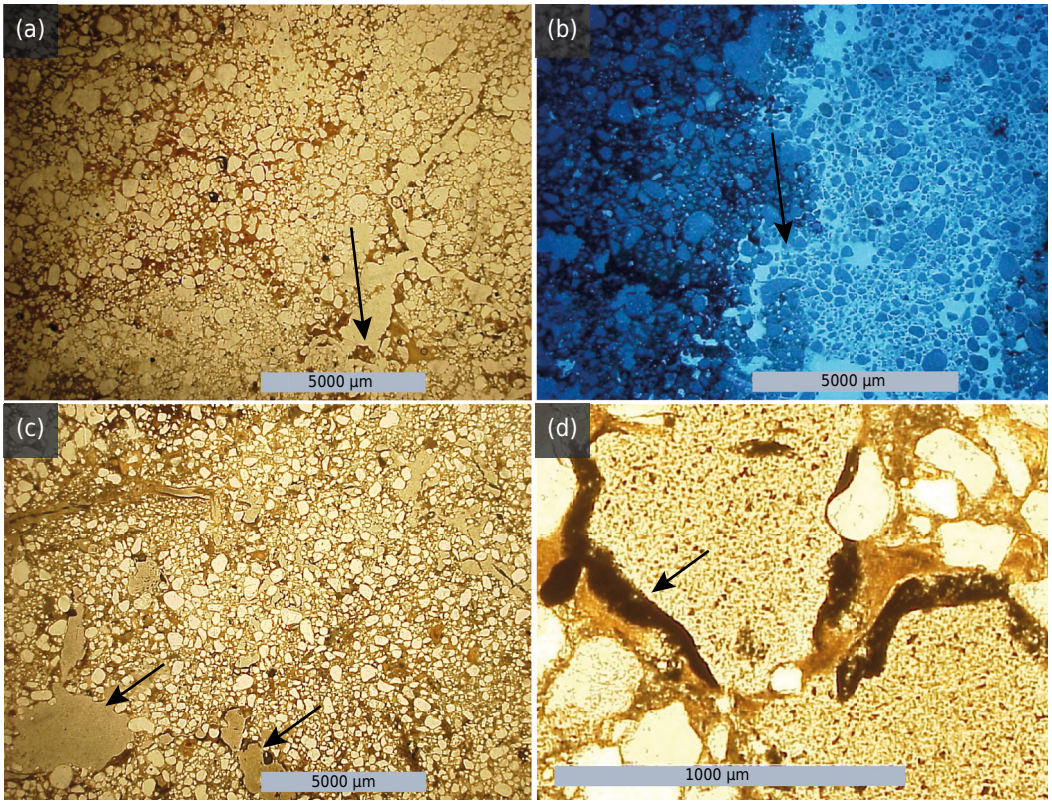

Figure 7. Photomicrograph of the 2Btgn1 horizons of P5; arrows indicating argilluviation (a), loss of clay and residual sand concentration (b), porphyritic texture with many ferrolysis dissolution/depletion cavities, and intense argilluviation, (c) pre-coalescence stage of the dissolution/depletion cavities: the presence of ferrans on the clay coatings is in agreement with the dynamics proposed by Brinkman (1970) for ferrolysis (d).

Table 5. Description of the thin section, according to Bullock et al. (1985) and Stoops (2003)

Sample	P1 - 2Btn	P2 - 2Btn1	P3 - 3Btnk	P4 - Btn1	P5 En/2Btgn	P5 - En/2Btgn
					Zone 1 - 2Btgn	Zone 2 - En
Microstructure	Chamber	Chamber	Subangular blocky	Massive	Massive	Spongy
Groundmass						
coarse material[(1)]	Quartz (100 %)	Quartz (100 %)	Quartz (95 %)	Quartz (100 %)	Quartz (100 %)	Quartz (100 %)
			Plagioclase (2 %)			
			Feldspar (2 %)			
			Biotite (1 %)			
Micromass	Undifferentiated	-	Speckled	Speckled	Undifferentiated	Undifferentiated
c/f related distribution[(2)]	Chitonic	Single spaced porphyric	Gefúrica	Close porphyric	Close porphyric	Concave gefuric
Pedofeatures	Clay coating	Fe hypocoating	Fe hypocoating	Clay coating	Fe hypocoating	Fe coatings
	Clay infilling	Clay infilling	Carbonate infilling		Fe-clay infilling	Mn coatings
	Fe hypocoating					

[(1)] Coarse material >2 mm. [(2)] c/f related distribution: coarse (>2 mm) and fine material (micromass) ratio.

Table 6. Classification of soils studied according to the Brazilian Soil Classification System (Santos et al., 2013), FAO (WRB, 2014) and Soil Taxonomy (Soil Survey Staff, 2014)

Profile	SiBCS	WRB	Soil Taxonomy
P1	*LUVISSOLO CRÔMICO Pálico abrúptico sódico*(1)	Abruptic Solonetz (Loamic, Cutanic, Magnesic, Hypernatric)	Typic Natrudalf
P2	*LUVISSOLO CRÔMICO Pálico abrúptico sódico*	Abruptic Solonetz (Loamic, Cutanic, Magnesic, Hypernatric)	Aquic Natrudalf
P3	*LUVISSOLO CRÔMICO Pálico planossólico sódico*(1)	Abruptic Stagnic Solonetz (Albic, Loamic, Cutanic, Magnesic, Hypernatric)	Aquic Natrudalf
P4	*LUVISSOLO CRÔMICO Pálico abrúptico sódico*(1)	Abruptic Stagnic Solonetz (Albic, Loamic, Cutanic, Magnesic, Hypernatric)	Aquic Natrudalf
P5	*PLANOSSOLO NÁTRICO Órtico espesso*	Abruptic Stagnic Solonetz (Albic, Loamic over Clayic, Cutanic, Magnesic, Hypernatric)	Glossic Natraqualf

(1) *Sódico*: character added to the fourth level as a new class.

considered for geomorphic classification. Together with the erosive process, the humid climate favors remobilization of some ions and compounds in the soil, such as carbonates. The carbonates were dated to a more recent period (660 years) and may be related to remobilization in the current wetter climate. During dissolution and reprecipitation in this climate, the new balance with the CO_2 of the soil promotes miscegenation between the older and newer C atoms.

In the relative distribution graph of the sand classes for the P3 and P5 profiles (Figure 4), there is no marked difference between the classes in the different horizons. On first analysis, this seems to refute the hypothesis of a textural gradient inherited by lithologic discontinuity. For the P2 profile, the distribution shows a differentiated pattern only in the subsurface horizons, where the first section of the B horizon (2Btn1) is probably formed by sedimentary packages, similar to the A and E horizons. Although it is located in one of the geomorphological units in a more advanced stage of dissection, the P4 profile had different sand distribution patterns in the Btn1 and Btn2 horizons. However, the 2Cgn horizon, at greater depth, had distribution similar to the A and E horizons.

Nevertheless, when using the criteria for lithologic discontinuity described by FAO (WRB, 2014), lithologic discontinuity can be observed in all the profiles (Table 4), exhibiting great variation among the sand proportions. The texture variations observed in paleolevee soils are largely inherited from sedimentary processes (Nascimento et al., 2013) and are dependent on the energy with which flooding occurs.

Considering the stages of topographic evolution described by Nascimento (2012), it can be observed that as the soils move to a more advanced stage of alteration, the E horizon increases its thickness to the detriment of the B horizon. This is evidenced by the irregular and tongue-shaped transition between both horizons (Figure 6), which is mandatory for identification of the natric horizon in Soil Taxonomy (Soil Survey Staff, 2014) and the FAO (WRB, 2014). The 2Btgn1 horizon of the P5 profile had a paler color (lower chroma) than the other profiles. This difference is related to the position of this profile in the flood plain of the São Lourenço River, which is situated at a lower elevation than the other profiles studied. Thus, even the soils of the highest part of the landscape, such as sodic soils, are affected by flooding more frequently than other geomorphic units and, consequently, oxidation and reduction processes are more intense, resulting in the paler color of the soil.

The high levels of basic cations may be the result of several cycles of concentration of the São Lourenço River floodwater, similar to those observed by Furquim et al. (2010a)

in the Nhecolândia Pantanal. Oliveira et al. (2009) and Parahyba et al. (2009) observed that the sodic character of the soils they studied in northeastern Brazil resulted from the incongruent dissolution of easily weathered primary minerals (van Breemen and Buurman, 2002). This hypothesis was rejected for the soils studied here, since the only profile which had easily weatherable primary minerals was the P3, and even so in amounts too small to confer a sodic character to the horizon.

Together with accumulation of ions, carbonate precipitation was observed in the P2 and P3 profiles, as well as formation of 2:1 clay minerals (Furquim et al., 2010b), which were present in all the B horizons of the profiles studied. The presence of both smectite and illite are mainly responsible for the strong grade of structures, ranging in size from medium to very large (Table 1), even though in some horizons the clay content does not exceed 350 g kg^{-1}. However, due to hydropedological change during the Holocene (Corradini and Assine, 2012; McGlue et al., 2012), with higher rainfall volumes and free drainage of the area, cations and anions were leached by direct precipitation and floodwater. Thus, the decrease in the EC and pH values from P1 to P5 suggests that the current environment favors sodification, that is, salt removal and Na^+ saturation in the exchange complex (Sumner and Naidu, 1998). In fact, ESP values increased from P1 to P5, the inverse of EC values, making the P4 and P5 profiles even more restrictive to plant development, which, in the field, caused an increase in the frequency of Acuri (*Attalea phalerata*).

The Al^{3+} contents were zero for most of the horizons analyzed, due to the high pH values that, in turn, favor precipitation of this cation as $Al(OH)_3$. The A horizon of the P4 profile and the A and 2Btgn2 horizons of the P5 profile showed Al^{3+} even with pH values in water slightly below 6.7, a condition where most soils from well drained areas have Al in the precipitate form. The presence of Al^{3+} at high pH values, together with Ca^{2+} values equal to zero, as observed in the 2Btgn2 horizon of the P5 profile, casts doubts on the differential thermodynamic equilibrium of this element in soils of the northern Pantanal. The Mg^{2+} values, often higher than those of Ca^{2+}, may be associated with alterations in clay minerals with Mg^{2+} in their structure, such as smectite, as observed in the XRDs (Ferreira et al., 2016b). They may also have been controlled by the formation of calcite ($CaCO_3$) in a sodic alkaline pathway (Al-Droubi et al., 1980), which is feasible under the chemical composition of the waters of the São Lourenço River (Rezende Filho et al., 2012). As carbonates are relatively easily soluble, in a more humid climate they are susceptible to dissolution and consequent removal of Ca^{2+} from the soil.

Unlike the results of Furquim et al. (2010a) and Furquim et al. (2010b), the diffractograms of the fine clay fraction of the Bt horizons showed a significant presence of kaolinite, evidenced by the reflection of plane *001* (0.71 nm). However, the asymmetry observed after solvation with ethylene glycol (Figure 5) suggests the interstratification of kaolinite-smectite (Moore and Reynolds, 1997), that is, part of the waves are reflected by the corresponding smectite phase. The presence of smectite-illite interlayers is also evidenced by the diffractograms, in which the samples saturated with Mg^{2+} showed a plane *001* reflection with great asymmetry towards larger angles (right of the peak). The observed interstratifications may be related to better drainage under current hydropedological conditions, where part of the K present between the layers of the illite is lost, becoming smectite (Bortoluzzi et al., 2005). Afterwards, as the process advances, part of the Si present in the siloxane layers is removed from the structure (desilication), resulting in the formation of the kaolinite phase of the interlayer (Bortoluzzi et al., 2007). Despite the significant presence of 2:1 clay minerals in the P5 profile, the low values of clay fraction activity are probably due to the higher proportion of coarse clay and its predominantly kaolinitic constitution (data not shown). The textural gradient observed in all the profiles studied causes deficient drainage in the profile, an effect that can be accentuated by the high levels of silt, as in the P2 and P4 profiles, for example. The predominance of the very fine and fine sand fractions is a consequence of the low energy sedimentary environment; both fractions contribute to the low hydraulic conductivity of the soil that, in turn, attenuates leaching.

The observations made in thin sections corroborate this hypothesis since the arrangements between the coarse and fine fractions are predominantly porphyric or gefuric, associated with the spongy or massive microstructure of the matrix (Bullock et al., 1985; Stoops, 2003), and none of them have substantial connectivity between the porous spaces. The abrupt transition between the En and 2Btgn1 horizons, observed in P5, results in the wide variation in the water saturation state in this region and the frequent alternations between Fe^{3+} and Fe^{2+}. This process, known as ferrolysis, acidifies the soil in a localized way and promotes the hydrolysis of some minerals, further accentuating the textural gradient (Brinkman, 1970; van Breemen and Burman, 2002).

The high ESP values associated with the lower values of electrical conductivity and Fe oxide content, which are important for flocculation of the colloids, make the clay fraction more prone to dispersion and, consequently, to translocation to greater depth. This process is shown by micromorphology, in which two zones are observed in the same thin section, one with a dense matrix (larger amount of plasma) and one with a less dense matrix (Figure 7b).

Even in the profiles where there is evidence of lithologic discontinuity, the process of argilluviation is identified in the thin section, as seen, for example, in the P2 profile, where there are signs of lithologic discontinuity. The clay coating features in the middle of the fractured carbonate nodule observed in the 2Btnk horizon (Figure 6) suggest that argilluviation is a current process. Therefore, it becomes difficult to distinguish how much of the gradient is inherited from the sedimentary processes and how much is the result of the current pedogenetic processes.

Classification

At the Order level, the result of the eluviation/illuviation process, such as the textural gradient and coating, was the most important aspect for classification in the three systems used. For the SiBCS, however, in addition to the textural gradient, the horizon color and clay activity were used for classification at the Order level, which differentiated the P5 class (*Planossolo*) from other profiles (*Luvissolo*). Considering only the Order level, Soil Taxonomy and the WRB did not make a distinction between the soils studied, while the SIBCS represented the soil alteration processes in a better manner, identifying the P5 in a different class. The classification of P5 as a *Planossolo* shows the intense clay eluviation/illuviation (abrupt textural change) and an internal drainage even more restricted than in the other profiles, reflected by the depletion of Fe oxides. In addition, Fe oxides are important in flocculation of soil colloids, and their absence or low content boost the dispersion and migration of the clay, evidenced by the thickening of the E horizon and a less dense matrix (Figure 7).

Although the SiBCS expressed differences in the pedogentic process in a more accurate manner at the Order level, it did not represent one of the most important characteristics of the soils studied. Sodic character was only represented in the *Planossolo*, at the Suborder level, and for the *Luvissolo*, it was not represented at the Great Group or at the Subgroup level. This limitation in the system was also pointed out by Oliveira et al. (2009) working with soils from the Northeast Region of Brazil, which shows that this situation is not exclusive to soils of the northern Pantanal. However, the SiBCS is an open system, enabling the user to add new classes at the fourth categorical level.

For the WRB, the sodic character is evidenced at the Order level as Solonetz, whereas in Soil Taxonomy, the character is considered at the Great Group level as Natrudalf, in all the profiles studied. As it exerts a significant influence on the physical and chemical properties of the soil, as well as on plant development, it would be of great importance to represent the sodic character in the *Luvissols* class, at least at the Great Group level, as is already the case for the *Gleissolos*, *Cambissolos*, *Neossolos*, and *Vertissolos*.

This use of the sodic character for discriminating the Great Groups of *Luvissolos* would be highly valuable for planning soil use and for formulating agricultural development

and conservation policies because the highest areas of the northern Pantanal are often associated with these soils and they are under heavy pressure from livestock during flood events, as well as serving as a refuge for wildlife.

CONCLUSIONS

Sodic soils of the northern Pantanal, formed in past hydropedological conditions, are currently subjected to clay eluviation/illuviation, ferrolysis, and leaching processes, though the last process mentioned is attenuated by the strong textural gradient.

The younger sodic soils in the region studied were classified as *Luvissolos* and, as the transformation process advances, depletion of iron oxides increases, along with clay eluviation, resulting in *Planossolos*.

Clay illuviation is the main pedogenetic process used in the three soil classification systems applied to the soils in this study. Together with ferrolysis, these processes show the stage of soil transformation. The high ESP values are considered by Soil Taxonomy at the Great Group level and by the WRB at the first level, whereas in the SiBCS, this characteristic discriminates one of the Suborders of the *Planossolos*, but it is not yet adequately addressed in the order of the *Luvissolos*.

Due to the restrictions imposed by high ESP and pH values on plant development, as well as their influence on soil physical properties and the dispersion capacity of soil clays, we suggest that the SiBCS adopt the sodic character in the third categorical level (Great Group) of *Luvissolos*, as is already the case for the *Gleissolos*, *Cambissolos*, *Neossolos*, and *Vertissolos*.

ACKNOWLEDGMENTS

The authors would like to thank FAPESP for financial support for projects 09/54372-0 and 11/11905-9 and the CNPq for the 201049/2012-0 grant. They also thank SESC Pantanal for logistical support during field activities, the staff of the Soil Laboratory of ESALQ/USP, and Dorival Grisotto, Luiz Antonio Silva Junior, and Sonia Aparecida de Moraes for field support, analytical activities, and thin section confection, respectively.

REFERENCES

Al-Droubi A, Fritz B, Gac JY, Tardy Y. Generalized residual alkalinity concept - application to prediction of the chemical evolution of natural waters by evaporation. Am J Sci. 1980;280:560-72. https://doi.org/10.2475/ajs.280.6.560

Anjos LHC, Jacomine PKT, Santos HG, Oliveira VA, Oliveira JB. Sistema brasileiro de classificação de solos. In: Ker JC, Curi N, Schaefer CEGR, Vidal-Torrado P, editores. Pedologia: fundamentos. Viçosa, MG: Sociedade Brasileira de Ciência do Solo, 2012. p.303-43.

Arnold RW. Concepts of soils and pedology. In: Wilding LP, Smeck NE, Hall GF, editors. Pedogenesis and soil taxonomy: I. Concepts and interactions. Amsterdam: Elsevier Science; 1983. p.1-21.

Assine ML, Soares PC. Quaternary of the Pantanal, west-central Brazil. Quat Int. 2004;114:23-34. https://doi.org/10.1016/S1040-6182(03)00039-9

Beirigo RM, Vidal-Torrado P, Stape JL, Couto EG, Andrade GRP. Solos da reserva particular do patrimônio natural SESC Pantanal. Rio de Janeiro: SESC, Departamento Nacional; 2011. Available at: http://www.sesc.com.br/portal/publicacoes/sesc/series_e_colecoes/conhecendo_o_pantanal_7/conhecendo_o_pantanal_7.

Bortoluzzi EC, Pernes M, Tessier D. Interestratificado caulinita-esmectita em um Argissolo desenvolvido a partir de rocha sedimentar do Sul do Brasil. Rev Bras Cienc Solo. 2007;31:1291-300. https://doi.org/10.1590/S0100-06832007000600008

Bortoluzzi EC, Santos DR, Kaminski J, Gatiboni LC, Tessier D. Alterações na mineralogia de um Argissolo do Rio Grande do Sul submetido à fertilização potássica. Rev Bras Cienc Solo. 2005;29:327-35. https://doi.org/10.1590/S0100-06832005000300002

Brinkman R. Ferrolysis, a hydromorphic soil forming process. Geoderma. 1970;3:199-206. https://doi.org/10.1016/0016-7061(70)90019-4

Bullock P, Fedoroff N, Jongerius A, Stoops G, Tursina T. Handbook for soil thin section description. London: Waine Research Publications; 1985.

Coelho IP. Do barro ao bamburro: relações entre a paisagem e a distribuição local de mamíferos e aves no Pantanal, Brasil [tese]. Porto Alegre: Universidade Federal do Rio Grande do Sul; 2016.

Corradini FA, Assine ML. Compartimentação geomorfológica e processos deposicionais no megaleque fluvial do rio São Lourenço, Pantanal mato-grossense. Rev Bras Geocienc. 2012;42:20-33. https://doi.org/10.5327/Z0375-75362012000500003

Corrêa MM, Ker JC, Mendonça ES, Ruiz HA, Bastos RS. Atributos físicos, químicos e mineralógicos de solos da região das Várzeas de Sousa (PB). Rev Bras Cienc Solo. 2003;27:311-24. https://doi.org/10.1590/S0100-06832003000200011

Donagema GK, Campos DVB, Calderano SB, Teixeira WG, Viana JHM, organizadores. Manual de métodos de análise do solo. 2a ed. rev. Rio de Janeiro: Embrapa Solos; 2011.

Ferreira EP, Anjos LHC, Pereira MG, Valladares GS, Cipriano-Silva R, Azevedo AC. Genesis and classification of soils containing carbonate on the Apodi Plateau, Brazil. Rev Bras Cienc Solo. 2016a;40:e0150036. https://doi.org/10.1590/18069657rbcs20150036

Ferreira JTP, Ribeiro Filho MR, Ribeiro MR, Souza Júnior VS, Bittar SMB, Santos RG. Planosols developed in different geoenvironmental conditions in northeastern Brazil. Rev Bras Cienc Solo. 2016b;40:e0150131. https://doi.org/10.1590/18069657rbcs20150131

Food and Agriculture Organization of the United Nations - FAO. Guidelines for soil description. 4th ed rev. Rome: FAO. 2006. Available at http://www.fao.org/docrep/019/a0541e/a0541e.pdf

Furquim SAC, Graham RC, Barbiero L, Queiroz Neto JP, Vidal-Torrado P. Soil mineral genesis and distribution in a saline lake landscape of Pantanal Wetland, Brazil. Geoderma. 2010a;154:518-28. https://doi.org/10.1016/j.geoderma.2009.03.014

Furquim SAC, Barbiéro L, Graham R, Queiroz Neto JP, Ferreira RPD, Furian S. Neoformation of micas in soils surrounding an alkaline-saline lake of Pantanal wetland, Brazil. Geoderma. 2010b;158:331-42. https://doi.org/10.1016/j.geoderma.2010.05.015

Gilardi JD, Duffey SS, Munn CA, Tell LA. Biochemical functions of geophagy in parrots: detoxification of dietary toxins and cytoprotective effects. J Chem Ecol. 1999;25:897-922. https://doi.org/10.1023/A:1020857120217

World Reference Base for Soil Resources - WRB: A framework for international classification, correlation and communication. Food and Agriculture Organization of the United Nations. Rome: IUSS/ISRIC/FAO; 2014. (World soil resources reports, 106)

Jackson ML. Soil chemical analysis: advanced course. Madison: Prentice-Hall; 1979.

Kämpf N, Curi N. Óxidos de ferro: Indicadores de atributos e ambientes pedogenênicos e geoquímicos. Tópic Cienc Solo. 2000;1:107-38.

Krasilnikov P, Arnold RW, Ibáñez JJ. Soil classifications: their origin, the state-of-the-art and perspectives. In: 19th World Congress of Soil Science, Soil Solutions for a Changing World. Brisbane; 2010. Published on DVD.

Landon, JR. Booker tropical soil manual: a handbook for soil survey and agricultural land evaluation in the tropics and subtropics. New York: Routledge; 1991.

Mcglue MM, Silva A, Zani H, Corradini FA, Parolin M, Abel EJ, Cohen AS, Assine ML, Ellis GS, Trees MA, Kuerten S, Gradella FS, Rasbold GG. Lacustrine records of Holocene flood pulse dynamics in the Upper Paraguay River watershed (Pantanal wetlands, Brazil). Quat Res. 2012;78:285-94. https://doi.org/10.1016/j.yqres.2012.05.015

Moore DM, Reynolds RC. X-Ray Diffraction and the identification and analysis of clay minerals. 2nd ed. Nova York: Oxford University Press, Oxford, 1997.

Murphy CP. Thin section preparation of soils and sediments. Berkhanmsterd: Academic Publis; 1986.

Nascimento AF. Relações pedologia-geomorfologia-sedimentologia no Pantanal Norte [tese] Piracicaba: Escola Superior de Agricultura Luiz de Queiroz; 2012.

Nascimento AF, Furquim SAC, Couto EG, Beirigo RM, Oliveira Junior JC, Camargo PB, Vidal-Torrado P. Genesis of textural contrasts in subsurface soil horizons in the Northern Pantanal-Brazil. Rev Bras Cienc Solo. 2013;37:1113-27. https://doi.org/10.1590/S0100-06832013000500001

Nascimento AF, Furquim SAC, Graham RC, Beirigo RM, Oliveira Junior JC, Couto EG, Vidal-Torrado P. Pedogenesis in a Pleistocene fluvial system of the Nothern Pantanal - Brazil. Geoderma. 2015;255-256:58-72. https://doi.org/10.1016/j.geoderma.2015.04.025

Oliveira LB, Fontes MPF, Ribeiro MR, Ker JC. Morfologia e classificação de Luvissolos e Planossolos desenvolvidos de rochas metamórficas no semiárido do nordeste brasileiro. Rev Bras Cienc Solo. 2009;33:1333-45. https://doi.org/10.1590/S0100-06832009000500026

Oliveira Junior JC, Melo VF, Souza LCP, Rocha HO. Terrain attributes and spatial distribution of soil mineralogical attributes. Geoderma. 2014;213:214-25. https://doi.org/10.1016/j.geoderma.2013.08.020

Oliveira Junior JC, Beirigo RM, Chiapini M, Nascimento AF, Couto EG, Vidal-Torrado P. Origin of mounds in the Pantanal wetlands: an integrated approach between geomorphology, pedogenesis, ecology and soil micromorphology. PLoS ONE. 2017;12:e0179197. https://doi.org/10.1371/journal.pone.0179197

Parahyba RBV, Santos MC, Rolim Neto FC. Evolução quantitativa de Planossolos do agreste do estado de Pernambuco. Rev Bras Cienc Solo. 2009;33:991-9. https://doi.org/10.1590/S0100-06832009000400023

Por FD. The Pantanal of Mato Grosso (Brazil): world's largest wetlands. 1st ed. Israel: Springer Netherlands; 1995. https://doi.org/10.1007/978-94-011-0031-1

Rengasamy P. Sodic soils. In: Lal R, Blum WH, Valentine C, Stewart BA, editors. Methods for assessment of soil degradation. Florida: CRC Press; 1997. p. 265-77.

Rezende Filho AT, Furian S, Victoria RL, Mascré C, Valles V, Barbiero L. Hydrochemical variability at the Upper Paraguay Basin and Pantanal wetland. Hydrol Earth Syst Sci. 2012;16:2723-37. https://doi.org/10.5194/hess-16-2723-2012

Santos HG, Jacomine PKT, Anjos LHC, Oliveira VA, Oliveira JB, Coelho MR, Lumbreras JF, Cunha TJF. Sistema brasileiro de classificação de solos. 3. ed. Rio de Janeiro: Embrapa Solos; 2013.

Silva CJ, Girard P. New challenges in the management of the Brazilian Pantanal and catchment area. Wetl Ecol Manage. 2004;12:553-61. https://doi.org/10.1007/s11273-005-1755-0

Soil Survey Staff. Keys to soil taxonomy. 12th ed. Washington, DC: United States Department of Agriculture, Natural Resources Conservation Service; 2014.

Stoops G. Guidelines for analyses and description of soil and regolith thin sections. Madison: Soil Society of America Inc; 2003.

Sumner ME, Naidu R. Sodic soils: distribution, properties, management, and environmental consequences. Oxford: Oxford University Press; 1998.

van Breemen N, Buurman P. Soil formation. 2nd ed. Dordrecht: Kluwer Academic Publishers, 2002.

Vidal-Torrado P, Lepsch IF, Castro SS, Cooper M. Pedogênese em uma seqüência Latossolo-Podzólico na borda de um platô na depressão periférica paulista. Rev Bras Cienc Solo. 1999;23:909-21. https://doi.org/10.1590/S0100-06831999000400018

Wallinga J, Murray A, Wintle A. The single-aliquot regenerative-dose (SAR) protocol applied to coarse-grain feldspar. Radiat Meas. 2000;32:529-33. https://doi.org/10.1016/S1350-4487(00)00091-3